NAVAL POSTGRADUATE SCHOOL
MONTEREY, CALIFORNIA

THESIS

ELECTROMAGNETIC RESONANCES OF METALLIC BODIES

by

William A. Lintz

June 1997

Thesis Co-Advisors: Richard W. Adler
Jovan E. Lebaric

DUDLEY KNOX LIBRARY
NAVAL POSTGRADUATE SCHOOL
MONTEREY CA 93943-5101

REPORT DOCUMENTATION PAGE

Form Approved OMB No. 0704-0188

1. AGENCY USE ONLY *(Leave blank)*	2. REPORT DATE June 1997	3. REPORT TYPE AND DATES COVERED Master's Thesis

4. TITLE AND SUBTITLE
ELECTROMAGNETIC RESONANCES OF METALLIC BODIES

5. FUNDING NUMBERS

6. AUTHOR(S) Lintz, William A.

7. PERFORMING ORGANIZATION NAME(S) AND ADDRESS(ES)
Naval Postgraduate School
Monterey CA 93943-5000

8. PERFORMING ORGANIZATION REPORT NUMBER

9. SPONSORING/MONITORING AGENCY NAME(S) AND ADDRESS(ES)

10. SPONSORING/MONITORING AGENCY REPORT NUMBER

11. SUPPLEMENTARY NOTES The views expressed in this thesis are those of the author and do not reflect the official policy or position of the Department of Defense or the U.S. Government.

12a. DISTRIBUTION/AVAILABILITY STATEMENT
Approved for public release; distribution is unlimited.

12b. DISTRIBUTION CODE

13. ABSTRACT *(maximum 200 words)*

Every object has the ability to radiate and scatter electromagnetic waves. The ability to predict frequencies of maximum radiation or scattering has been limited to simple objects, such as dipoles, or objects with high degrees of symmetry. This thesis describes modifications that can be made to a computational electromagnetic technique, the Method of Moments, to allow for such predictions to be made for complex metallic objects. This new technique has been implemented as a MATLAB computer program and tested on objects with known resonance frequencies. Finally, the code's ability to handle large complex objects is demonstrated by investigating the resonance frequencies for a Cessna aircraft.

14. SUBJECT TERMS Natural Resonance Frequency, Natural Frequency Modes, Eigen Analysis, Electromagnetic Radiation Waves

15. NUMBER OF PAGES 56

16. PRICE CODE

17. SECURITY CLASSIFICATION OF REPORT	18. SECURITY CLASSIFICATION OF THIS PAGE	19. SECURITY CLASSIFICATION OF ABSTRACT	20. LIMITATION OF ABSTRACT
Unclassified	Unclassified	Unclassified	UL

NSN 7540-01-280-5500

Standard Form 298 (Rev. 2-89)
Prescribed by ANSI Std. 239-18 298-102

ELECROMAGNETIC RESONANCES OF METALLIC BODIES

William A. Lintz
Lieutenant, United States Navy
B.E.E., Villanova University, 1992

Submitted in partial fulfillment of the
requirements for the degree of

MASTER OF SCIENCE IN ELECTRICAL ENGINEERING

from the

NAVAL POSTGRADUATE SCHOOL
June 1997

ABSTRACT

Every object has the ability to radiate and scatter electromagnetic waves. The ability to predict frequencies of maximum radiation or scattering has been limited to simple objects, such as dipoles, or objects with high degrees of symmetry. This thesis describes modifications that can be made to a computational electromagnetic technique, the Method of Moments, to allow for such predictions to be made for complex metallic objects. This new technique has been implemented as a MATLAB computer program and tested on objects with known resonance frequencies. Finally, the code's ability to handle large complex objects is demonstrated by investigating the resonance frequencies for a Cessna aircraft.

TABLE OF CONTENTS

I. INTRODUCTION AND BACKGROUND

A. RESEARCH FOCUS

Electromagnetic waves interact with all objects in space but differently at different frequencies. For example, the physical dimensions of an antenna, such as the length of a dipole or the diameter of a circular horn, determine the frequency range of antenna operation. Any metallic object can operate as an efficient antenna at a number of frequencies. These frequencies can be referred to as the resonance frequencies or the eigen frequencies of the object. The eigen frequencies can be determined analytically for metallic bodies of simple shape or for objects with high degrees of symmetry. The eigen frequencies for complex bodies must be determined numerically, using computer implemented algorithms. The purpose of finding the eigen frequencies of complex metallic objects is to determine the optimal frequencies for their use as antennas or to determine optimal frequencies for their detection as radar targets. [Ref. 1] The starting point for algorithm development is the well established Method of Moments (MOM). This technique leads to a matrix equation which may then be used to formulate an electromagnetic eigen-value problem.

This chapter provides mathematical and conceptual background for the MOM technique. Chapter II explains the modifications of the MOM to formulate the algebraic eigen-value problem whose solution provides the resonance frequencies of the object. Chapter III explains the implementation of the eigen theory into a MATLAB computer program and verifies the code for an object with known resonance frequencies. Chapter

IV shows examples of the code's use for eigen analysis of complex objects. Finally, Chapter V presents conclusions and recommendations for further research.

B. ELECTROMAGNETIC AND MATHEMATICAL BACKGROUND

The Method of Moments is a numerical technique used to solve integral equations which describe electromagnetic interactions for radiation and scattering problems. The integral equations are set up to solve for the surface current densities induced on an object due to a source. Once the theoretical equations have been formulated, the MOM can be applied by discretizing and solving the problem using matrix techniques.

Applying the MOM technique [Ref. 2] to a single wire provides the building block needed to consider more complex objects. MOM creates a discrete model of the object by dividing the object into electrically small charge and current segments referred to as the "basis." The amplitudes of these basis functions are not known and need to be determined. The MOM result is a series of basis functions that approximates the actual surface current distribution. Complex metallic objects can be approximated using wire grid models, assuming that the surface current densities only vary longitudinally along the wires and do not vary circumferentially. The currents at the ends of connected and non-connected wires are of particular interest. The currents at non-connected segment ends can be assumed zero, and the currents at the wire ends forming a junction should satisfy Kirchoff's Current Law (KCL).

Once the wire has been segmented, as demonstrated in (Fig. 1-1), discrete equations can be formulated directly from the physical layout of the problem.

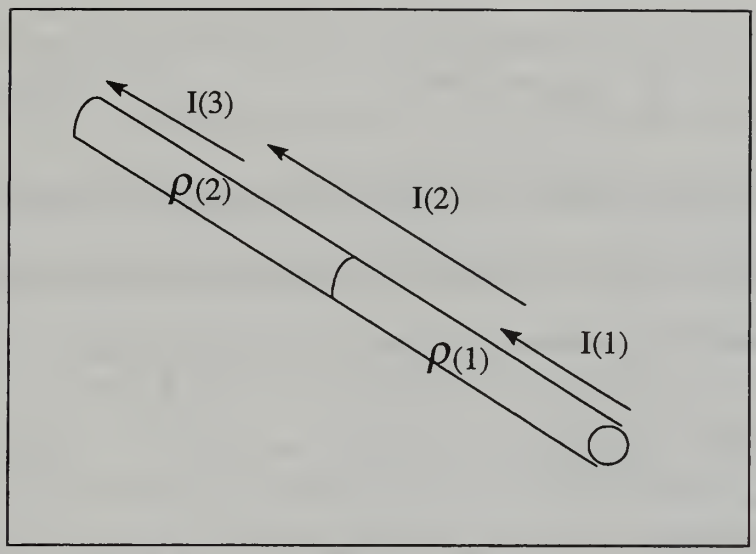

Figure (Fig. 1-1), Example of a segmented wire

The expressions for the electric and magnetic potentials ("mixed potential" MOM formulation), make up the building block equations, and for any problem they can be written as:

$$\Phi(m) = \frac{1}{\varepsilon}\sum_{n=1}^{N_q}\rho(n)K_\Phi(m,n) \qquad \text{(Eq. 1-1)}$$

$$A(m) = \mu\sum_{n=1}^{N_i}I(n)K_A(m,n) \qquad \text{(Eq. 1-2)}$$

where the K's represent Green's function integrals (shown below), ρ (n) represents line charge density, I(n) represents current, A(m) represents magnetic potential, Φ(m) represents electric potential, μ represents permeability, ε represents permittivity, N_i

represents the total number of current segments and N_q represents the total number of charge segments.

$$K = \int_{\zeta_{low}}^{\zeta_{high}} \frac{e^{-jk|\bar{r}-\bar{r}'(\zeta)|}}{4\pi|\bar{r}-\bar{r}'|} d\zeta \qquad \text{(Eq. 1-3)}$$

ζ represents the z position of the segment in local coordinates, and k is the wavenumber. The difference between K_Φ and K_A is in integral limits and location of observation points, as will be seen in Chapter II. In addition, the equation of continuity is used:

$$\rho(n) = \frac{-1}{j\omega\Delta l_q(n)}(I(n+qw_n) + I(n+qw_n-1)) \qquad \text{(Eq. 1-4)}$$

where n denotes a source point, m denotes an observation point and qw_n denotes the number of the wire to which the n-th source point belongs. The term $\Delta l_q(n)$ represents the length of a charge segment, and ω denotes the angular frequency. By substitution, (Eq. 1-1) and (Eq. 1-4) may be combined to provide an electric scalar potential equation relying solely on current, as shown in (Eq. 1-5):

$$\Phi(m) = \frac{1}{j\omega\varepsilon}\left[\sum_{n=1}^{N_q} \frac{1}{\Delta l_q(n)}(I(n+qw_n) - I(n+qw_n-1))K_\Phi(m,n)\right].$$

(Eq. 1-5)

By combining the tangential component of the electric field due to current, (Eq. 1-2), and the gradient of electric scalar potential along the observed wire, an expression can be formed for the total tangential electric field at the n-th observation point as:

$$E(m) = \frac{1}{j\omega\varepsilon\Delta l_i(m)}\left[\sum_{n=1}^{N_q} \frac{1}{\Delta l_q(n)}(I(n+qw_n) - I(n+qw_n-1))(K_\Phi(m-iw_m+1,n) - K_\Phi(m-iw_m,n)\right]$$

$$- j\omega\mu \sum_{n=1}^{N_i} I(n) K_A(m,n) \qquad \text{(Eq. 1-6)}$$

where $\Delta l_i(m)$ represents the length of a current segment. By requiring that the voltage, $E(m)\Delta l(i_m)$, be equal to the negative of the source voltage, (Eq. 1-6) can be rewritten to provide equations which are functions of source voltage. (Eq. 1-6) can then be written as a single sum using arrays to identify wire ends (start and stop):

$$V(m) = \sum_{n=1}^{N_i} \left[Z_{term1} + Z_{term2} \cdot start(n) - Z_{term3} \cdot stop(n) \right] I(n) \qquad \text{(Eq. 1-7)}$$

where the equation has been simplified by the use of $Zterm1$, $Zterm2$ and $Zterm3$. These can be written explicitly as:

$$Z_{term1} = j60\pi \left(\frac{\Delta l_i(m)}{\lambda} \right) K_A(m,n) \qquad \text{(Eq. 1-8)}$$

$$Z_{term2} = -j \frac{30}{2\pi} \frac{\lambda}{\Delta l_q(n - iw_n + 1)} \left(K_\Phi(m - iw_m + 1, n - iw_n + 1) - K_\Phi(m - iw_m, n - iw_n + 1) \right)$$

(Eq. 1-9)

$$Z_{term3} = -j \frac{30}{2\pi} \frac{\lambda}{\Delta l_q(n - iw_n)} \left(K_\Phi(m - iw_m + 1, n - iw_n) - K_\Phi(m - iw_m, n - iw_n) \right)$$

(Eq. 1-10)

where λ is the operating wavelength. The system of equations, (Eq. 1-7), can be written in a matrix form:

$$[Vm] = [Zm,n][In]. \qquad \text{(Eq. 1-11)}$$

Once the Z terms have been formed and the source voltage is specified, the surface currents on the wire can be found as:

$$[I] = \left[Z^{-1}\right] \cdot [V]. \qquad \text{(Eq. 1-12)}$$

For a system of equations written in matrix form, there is a special source-less solution. This is referred to as the eigen problem:

$$[Z] \cdot \vec{I} = \lambda \cdot \vec{I} \qquad \text{(Eq. 1-13)}$$

where λ represents the eigen values of the matrix Z and I represents the associated eigen vectors (eigen currents).

Using the concepts described above and Kirchoff's Current and Voltage Laws, the concept of eigen frequencies can be introduced. In the next chapter, the techniques for MOM modeling and matrix manipulation will be applied to form the basis for finding eigen frequencies of metallic bodies of arbitrary shape.

II. MOM MODELING AND THE EIGEN SOLUTION

A. ELECTROMAGNETIC MODELING

The last chapter provided background in MOM electromagnetic modeling. This background is important because of the need to initially define a problem in electromagnetic terms. Once this step has been accomplished, an effort to manipulate the model for the purpose of finding the eigen solution can be attempted.

The initial problem in creating a MOM model for a metallic structure is an acceptable wire grid model of the object. This process involves the formulation of a structure that adequately simulates the shape of the original object without defining a problem which is too large to be solved on a computer. This concept will be dealt with more in a later chapter involving computer coding of the theoretical results. It will be assumed that a wire model for a metallic object has been created in order to begin the building toward the eigen solution.

A wire grid model of an object can be assembled using a number of straight wires. These wires can then be treated individually, and the effects of current and charge on each wire can be summed at selected observation points. The first step in this process is to use (Eq. 1-1), (Eq. 1-2) and (Eq.1-4) to formulate the expressions based on imposing the boundary condition of vanishing tangential electric field on the surface of each wire. Consider the electric field contributions by the electric scalar potential and magnetic vector potential separately:

$$V_s(m) = E_s(m)\Delta l_i(m) = \Phi(m) - \Phi(m-1) \qquad \text{(Eq. 2-1)}$$

$$V_A(m) = E_A(m)\Delta l_i(m). \qquad \text{(Eq. 2-2)}$$

The voltage across each segment can then be considered as a sum of three terms. One is due to the gradient of the electric scalar potential. The second is due to the time variation of the magnetic vector potential, and the third is due to voltage sources. The sum of these three components must cancel to zero due to the imposition of PEC boundary conditions of vanishing tangential electric field on the wire surface. The sum can be written as:

$$-V_\Phi(m) - V_A(m) = V_s(m) \qquad \text{(Eq. 2-3)}$$

where $V_s(m)$ represents source voltage. The expressions for V_A and V_Φ can then be substituted into the above equation and manipulated to group like terms for a formulation that resembles (Eq. 1-11).

B. EIGEN PROBLEM FORMULATION

The matrix equation, (Eq. 1-11), applies to the case of an object driven by a source voltage vector, V_s. By setting the source voltage vector to zero, a solution can be found which does not depend on the source voltage input. The solution for the source-less problem is referred to as the eigen problem solution. The eigen problem solution has two components: a set of eigen values and a corresponding set of eigen vectors. The eigen problem formulation also involves approximations related to evaluation of Green's functions integrals in closed form and implementation of wire junction conditions.

1. Simplification

To manipulate the equations for the MOM problem into the form of an algebraic eigen problem, some simplifications and approximations are required. First, by multiplying the equations by jωεΔl (where Δl is the average charge segment length), the concept of a normalized wavenumber can be introduced. The normalized wavenumber,κ, is defined as:

$$\omega^2\mu\varepsilon\Delta l^2 = \left(\frac{\omega}{v_o}\right)^2 \Delta l^2 = (k\Delta l^2) = \kappa^2 \qquad \text{(Eq. 2-4)}$$

where v_o represents the velocity of propagation in the medium. Similarly we can express:

$$j\omega\varepsilon\Delta l = j\omega\sqrt{\mu\varepsilon}\,\frac{1}{\sqrt{\frac{\mu}{\varepsilon}}}\Delta l = j\kappa Y_o \qquad \text{(Eq. 2-5)}$$

and introduce a new "scaled" vector of unknown end "voltages:"

$$\psi_{end}(n) = \kappa Y_o V_{end}(n) \qquad \text{(Eq. 2-6)}$$

where Y_o is the intrinsic admittance of free space. The MOM equations can now be written in a simpler form using the above notation. The sample equations below are given for a straight wire with two charge segments as shown in (Fig. 1-1):

$$(K_\Phi(1,1) - K_\Phi(2,1))I_1 + (K_\Phi(1,2) - K_\Phi(1,1) + K_\Phi(2,1) - K_\Phi(2,2))I_2 + (K_\Phi(2,2) - K_\Phi(1,2))I_3$$

$$+\kappa^2 \frac{\Delta l}{\Delta l_2}(K_A(2,1)I_1 + K_A(2,2)I_2 + K_A(2,3)I_3) = 0 \qquad \text{(Eq. 2-7)}$$

with the ends represented as:

$$-K_{\Phi}(1,1)I_1+(K_{\Phi}(1,1)-K_{\Phi}(1,2))I_2+K_{\Phi}(1,2)I_3$$

$$+\kappa^2\frac{\Delta l}{\Delta l_1}(K_A(1,1)I_1+K_A(1,2)I_2+K_A(1,3)I_3)+\psi_{end1}=0 \qquad \text{(Eq. 2-8)}$$

$$-K_{\Phi}(2,1)I_1+(K_{\Phi}(2,1)-K_{\Phi}(2,2))I_2+K_{\Phi}(2,2)I_3$$

$$+\kappa^2\frac{\Delta l}{\Delta l_3}(K_A(3,1)I_1+K_A(3,2)I_2+K_A(3,3)I_3)+\psi_{end2}=0. \qquad \text{(Eq. 2-9)}$$

In the above equations the K's represent Green's function integrals. These equations illustrate the starting point for the MOM eigen analysis. The next step is to evaluate the K terms. The following section explains the approximations used to simplify the Green's functions such that numerical integration is avoided.

2. Green's Function Integral Evaluation

The Green's function integrals do not have closed form solutions over wire segments and in general must be evaluated numerically. However, if the Green's function is first approximated using Taylor series expansion, the integrals approximate the exact answer and a closed form solution does exist. Therefore, we first expand the Green's function into a Taylor series using:

$$\frac{e^{-jk(|\vec{r}-\vec{r}'|-r_o)}}{4\pi\cdot|\vec{r}-\vec{r}'|}\cdot e^{-jkr_o}=\frac{1}{4\pi}\frac{1-jk(|\vec{r}-\vec{r}'|-r_o)}{|\vec{r}-\vec{r}'|}\cdot e^{-jkr_o}=\frac{e^{-jkr_o}}{4\pi}\left[(1+jkr_o)\frac{1}{|\vec{r}-\vec{r}'|}-jk\right].$$

(Eq. 2-10)

The above expression can be simplified by introducing the normalized wavenumber κ.

$$\frac{e^{-jk(|\vec{r}-\vec{r}'|-r_o)}}{4\pi|\vec{r}-\vec{r}'|}\cdot e^{-jkr_o} = \frac{e^{-j\kappa\left(\frac{r_o}{\Delta l}\right)}}{4\cdot\pi}\left[\left[1+j\kappa\left(\frac{r_o}{\Delta l}\right)\right]\frac{1}{|\vec{r}-\vec{r}'|}-j\kappa\frac{1}{\Delta l}\right]$$

(Eq. 2-11)

In order to remove the wavenumber from the exponential, a further approximation needs to be made. The value of r_o represents the distance between the source and the observation points. The terms with the largest magnitude are the "self terms," for which the source and observation points are the same and r_o=0. Therefore, setting r_o=0 introduces no error for the terms that are the largest in magnitude, but phase errors are introduced when the observation point is moved away from the source point. Fortunately, the magnitude of the Green's function decreases as the phase error increases. This causes the influence of the phase error to decrease as r_o increases. Therefore, we can approximate the Green's function by:

$$\frac{1}{4\pi}\left(\frac{1}{|\vec{r}-\vec{r}'|}-j\kappa\frac{1}{\Delta l}\right).$$

(Eq. 2-12)

The integrals for the approximated Green's function can then be simplified by splitting them into real and imaginary parts:

$$K_\Phi(m,n) = K_{\Phi r}(m,n) - j\cdot\kappa\cdot K_{\Phi i}(m,n)$$

(Eq. 2-13)

$$K_A(m,n) = K_{Ar}(m,n) - j\cdot\kappa\cdot K_{Ai}(m,n)$$

(Eq. 2-14)

where the electric potential K terms represent the integrals of the Green's function over the n-th charge segment, and the magnetic potential K terms represent the integrals of the

Green's function over the n-th current segment. Each of the Green's function integrals can be explicitly written as:

$$K_V(m,n)=\int_{\zeta_{low(n)}}^{\zeta_{high(n)}}\frac{1}{\sqrt{\left[x_m-(u_\zeta a+x_n+u_{\zeta x}\zeta)\right]^2+\left[y_m-(u_\zeta a+y_n+u_{\zeta y}\zeta)\right]^2+\left[z_m-(u_\zeta a+z_n+u_{\zeta z}\zeta)\right]^2}}d\zeta$$

(Eq. 2-15)

$$K_{Ai}(m,n)=\int_{\zeta_{low(n)}}^{\zeta_{high(n)}}1\cdot d\zeta=\zeta_{high(n)}-\zeta_{low(n)}$$

(Eq. 2-16)

$$K_{\Phi}(m,n)=\int_{\zeta_{low(n)}}^{\zeta_{high(n)}}\frac{1}{\sqrt{\left[x_{c(m)}-(u_\zeta a+x_{c(n)}+u_{\zeta x}\zeta)\right]^2+\left[y_{c(m)}-(u_\zeta a+y_{c(n)}+u_{\zeta y}\zeta)\right]^2+\left[z_{c(m)}-(u_\zeta a+z_{c(n)}+u_{\zeta z}\zeta)\right]^2}}d\zeta$$

(Eq. 2-17)

$$K_{\Phi i}(m,n)=\int_{\zeta_{low(n)}}^{\zeta_{high(n)}}1\cdot d\zeta=\zeta_{high(n)}-\zeta_{low(n).}$$

(Eq. 2-18)

Introducing:

$$A=x_m-x_n-u_{\zeta x}\cdot a$$

(Eq. 2-19)

$$B=u_{\zeta x}$$

(Eq. 2-20)

$$C=y_m-y_n-u_{\zeta y}\cdot a$$

(Eq. 2-21)

$$D=u_{\zeta y}$$

(Eq. 2-22)

$$E=z_m-z_n-u_{\zeta z}\cdot a$$

(Eq. 2-23)

$$F = u_{\zeta}$$

(Eq. 2-24)

the denominators of the real parts of the approximated Green's function integrals can be expressed as:

$$(A-B\zeta)^2+(C-D\zeta)^2+(E-F\zeta)^2=(B^2+D^2+F^2)\zeta^2+(-2(AB+CD+EF))\zeta+(A^2+C^2+E^2).$$

(Eq. 2-25)

Realizing that the first expression on the right hand side of this equation, $B^2+D^2+F^2$, represents the addition of the squares of the orthogonal components of the unit vectors for the wire, its value is equal to 1. The 1/r integrals can then be written as:

$$K=\int_{\alpha}^{\beta}\frac{1}{\sqrt{\zeta^2-2(AB+CD+EF)\zeta+(A^2+C^2+E^2)}}d\zeta.$$

(Eq. 2-26)

The solution to an integral of this form depends on the determinant of the quadratic equation in the denominator:

$$Det=4\left[(AB+CD+EF)^2-(A^2+C^2+E^2)\right].$$

(Eq. 2-27)

If the value of this determinant is zero, the analytic solution to the integral is:

$$K=\ln\left[\frac{\beta-(AB+CD+EF)}{\alpha-(AB+CD+EF)}\right]$$

(Eq. 2-28)

otherwise:

$$K=\ln\left[\frac{\sqrt{(A-B\beta)^2+(C-D\beta)^2+(E-F\beta)^2}+\beta-(AB+CD+EF)}{\sqrt{(A-B\beta)^2+(C-D\beta)^2+(E-F\beta)^2}+\alpha-(AB+CD+EF)}\right].$$

(Eq. 2-29)

The analytic solutions will be used in formulating the algebraic eigen value problem.

3. KCL and KVL

In order to form structures involving more wires, the concept of wire connection needs to be addressed. It was discussed in Chapter I how the current for the free ends of a wire will be assumed zero for a MOM formulation. When wires are connected, the currents of the junction need to satisfy KCL (the sum of all the currents into the junction equals zero), and the end potentials at each of the joined wire ends must be equal (KVL). To account for KCL and KVL, augmentation matrices can be introduced:

$$D \cdot I = 0 \qquad \text{(Eq. 2-30)}$$

$$F \cdot \psi = 0 \qquad \text{(Eq. 2-31)}$$

where the D matrix represents KCL connections, and the F matrix indicates KVL in the structure. As an example, KCL for a single wire with three charge segments, as shown in (Fig. 1-1) would be represented by:

$$D = \begin{bmatrix} -1 & 0 & 0 & 0 \\ 0 & 0 & 0 & 1 \end{bmatrix}. \qquad \text{(Eq. 2-32)}$$

The KVL matrix would be empty for this example, since there are no wire connections, but a three wire junction would produce the following KVL matrix:

$$F = \begin{bmatrix} 1 & -1 & 0 \\ 1 & 0 & -1 \end{bmatrix}. \qquad \text{(Eq. 2-33)}$$

4. Eigen Solution

Returning to the MOM equations with the normalized wavenumber notation, (Eq. 2-4), as demonstrated in (Eq. 2-7), (Eq. 2-8) and (Eq. 2-9), we can write the MOM equations in matrix format as:

$$\kappa^2 AI + BI + jC\psi = 0. \qquad \text{(Eq. 2-34)}$$

This system is then augmented by the KCL and KVL equations defined in (Eq. 2-30) and (Eq. 2-31). To further simplify the matrix equations, normalized wavelength will be introduced:

$$\nu = \frac{1}{\kappa}. \qquad \text{(Eq. 2-35)}$$

Implementing the approximation for the Green's function integrals, (Eq. 2-13) and (Eq. 2-14), the matrix equation, (Eq. 2-34), can be written as:

$$(A_r - j\frac{1}{\nu}A_i)I + \nu^2(B_r - j\frac{1}{\nu}B_i)I + jC\nu^2\psi = 0. \qquad \text{(Eq. 2-36)}$$

This simplifies to:

$$\nu^3 B_r I - j\nu^2 B_r I + \nu A_r I - jA_r I + j\nu^3 C\psi = 0. \qquad \text{(Eq. 2-37)}$$

Grouping terms with like powers of normalized wavelength, we get:

$$\nu^3\begin{bmatrix} B_r & jC \\ D & 0 \\ 0 & F \end{bmatrix}\begin{pmatrix} I \\ \psi \end{pmatrix} - j\nu^2\begin{bmatrix} B_i & 0 \\ 0 & 0 \end{bmatrix}\begin{pmatrix} I \\ \psi \end{pmatrix} + \nu\begin{bmatrix} A_r & 0 \\ 0 & 0 \end{bmatrix}\begin{pmatrix} I \\ \psi \end{pmatrix} - j\begin{bmatrix} A_i & 0 \\ 0 & 0 \end{bmatrix}\begin{pmatrix} I \\ \psi \end{pmatrix} = 0. \qquad \text{(Eq. 2-38)}$$

We can annotate the individual matrices as:

$$br = \begin{bmatrix} B_r & j \cdot C \\ D & 0 \\ 0 & F \end{bmatrix} \qquad \text{(Eq. 2-39)}$$

$$bi = \begin{bmatrix} B_i & 0 \\ 0 & 0 \end{bmatrix} \qquad \text{(Eq. 2-40)}$$

$$ar = \begin{bmatrix} A_r & 0 \\ 0 & 0 \end{bmatrix} \qquad \text{(Eq. 2-41)}$$

$$ai = \begin{bmatrix} A_i & 0 \\ 0 & 0 \end{bmatrix}. \qquad \text{(Eq. 2-42)}$$

Note that matrices br, bi, ar and ai are all square and equal in size. Now the matrix equation, (Eq. 2-38), is pre-multiplied by the inverse of br:

$$inv(br) = \begin{pmatrix} \beta_1 & \beta_2 \\ \beta_3 & \beta_4 \end{pmatrix}. \qquad \text{(Eq. 2-43)}$$

Since matrices bi, ar and ai have no terms in the (1,2), (2,1) and (2,2) position, the result of the pre-multiplication by the inverse is:

$$v^3(Identity)\begin{pmatrix} I \\ \psi \end{pmatrix} - jv^2\begin{bmatrix} \beta_1 \cdot B_i & 0 \\ \beta_3 \cdot B_i & 0 \end{bmatrix}\begin{pmatrix} I \\ \psi \end{pmatrix} + v\begin{bmatrix} \beta_1 \cdot A_r & 0 \\ \beta_3 \cdot A_r & 0 \end{bmatrix}\begin{pmatrix} I \\ \psi \end{pmatrix} - j\begin{bmatrix} \beta_1 \cdot A_i & 0 \\ \beta_3 \cdot A_i & 0 \end{bmatrix}\begin{pmatrix} I \\ \psi \end{pmatrix} = 0.$$

(Eq. 2-44)

Recognizing that this is a current (I) and "voltage" (ψ) formulation and that a solution for currents only is sufficient and smaller in size, only the upper "half" of the matrix equation that involves the current, I, needs to be retained:

$$(v^3 - jv^2\beta_1 B_i + v\beta_1 A_r - j\beta_1 A_i)I = 0. \qquad \text{(Eq. 2-45)}$$

A solution for the normalized wavelength can be obtained from this equation, but in order to do this, auxiliary vectors need to be introduced to linearize the cubic eigen problem. These vectors can be represented as:

$$I_1 = \nu \cdot I \qquad \text{(Eq. 2-46)}$$

and

$$I_2 = \nu \cdot I_1 \qquad \text{(Eq. 2-47)}$$

These vectors can be included in the system of equations, producing:

$$\nu I_2 - j\beta_1 B_i I_2 + \beta_1 A_r I_1 - j\beta_1 A_i I = 0. \qquad \text{(Eq. 2-48)}$$

Combining (Eq. 2-46), (Eq. 2-47) and (Eq. 2-48) a "super-matrix" equation can be formed:

$$\begin{bmatrix} j\beta_1 B_i & -\beta_1 A_r & j\beta_1 A_i \\ 1 & 0 & 0 \\ 0 & 1 & 0 \end{bmatrix} \begin{bmatrix} I_2 \\ I_1 \\ I \end{bmatrix} = \nu \begin{bmatrix} I_2 \\ I_1 \\ I \end{bmatrix}. \qquad \text{(Eq. 2-49)}$$

Or written simply as:

$$A_{sup} \cdot I = \nu \cdot I. \qquad \text{(Eq. 2-50)}$$

The above is recognized as the standard algebraic eigen problem form as introduced in (Eq. 1-13). Values for the normalized wavelength can be found using a standard algebraic eigen solver. The normalized wavelengths can then be transformed into wavelengths and frequencies using the relationships:

$$\nu = \frac{\lambda}{2\pi\Delta l} \qquad \text{(Eq. 2-51)}$$

and

$$f = \frac{v_o}{\lambda}. \qquad \text{(Eq. 2-52)}$$

The eigen frequencies are the frequencies where the structure is electromagnetically resonant. Each frequency has an associated eigen vector, which represents the current distribution for the particular resonance frequency ("mode"). In order to obtain the eigen frequencies and eigen currents, the theory must be implemented in a computer code. The next chapter will describe the code to define and solve the eigen problem and discuss its results.

III. IMPLEMENTATION AND TESTING

A. COMPUTER IMPLEMENTATION

The previous chapter showed that it is possible, with the introduction of certain approximations, to obtain the electromagnetic resonance frequencies for metallic objects modeled as collections of thin wires. It is not feasible to implement the eigen problem "by hand" due to its size. The eigen problem formulation and solution need to be implemented on a computer. In a computer implementation of the eigen formulation additional issues must be considered. These will be explained in this section where the coding process of the eigen problem is discussed. Once the code has been developed, it can be tested for several objects whose resonant frequencies can be obtained analytically. This testing will help to determine coding accuracy and the magnitudes of errors introduced by the approximations made in formulating the eigen problem.

Prior to coding the problem, an overall strategy must be determined. The matrix form of the eigen problem suggests MATLAB as a natural choice for coding. With MATLAB the elements of the computer implementation process can be addressed, such as: entering the problem geometry and defining wire segments, matrix assembly, implementing KCL and KVL, and the super-matrix "fill." Finally, the solution and display of eigen currents and the associated far-fields will be discussed.

1. Object Geometry Definition

The eigen program can not be run until an object is defined. In the case of the eigen problem, a number of parameters are necessary to provide the algorithm with all of

the information pertinent to the solution process, such as the physical dimensions and orientation of each wire.

Each wire is assumed to have a cylindrical shape defined by the wire length and radius. It is important to note that the MOM model, as defined in Chapter I, requires wire length to be much greater than its radius and segment length to be larger than the radius as well ("thin wire" assumption) for an accurate solution. The wire grid model should be created with this in mind. Another important consideration for the construction of the wire model is the number of segments per wire. For good accuracy the MOM model requires about ten samples per operating wavelength. The average segment length thus defines the upper frequency limit for which an accurate eigen solution can be found. It is assumed that wires are made of good conductors, defined by their permeability and conductivity. In addition, lumped elements (resistors, capacitors and inductors) can be added to the whole wire or some of its segments.

Wire position is defined with respect to "global" Cartesian coordinates. A "local" coordinate system is defined for each wire to simplify the MOM implementation. The set of local coordinates needs to be transformed to the global coordinates to account for the interaction with other wires. This local to global coordinate transformation is accomplished by rotation and translation of the local coordinate system. The transformed local coordinates can be used to determine the distances between points on the wire surface and arbitrary observation points away from the wire.

As each wire is entered, it can be identified within the program by a designated wire number. The charge and current pulses associated with each of these wires can then

be identified by their wire number and their individual pulse number on the wire. Individual assignments of directional unit vectors can be made for each wire segment.

Now that the geometry and segmentation of the wires has been defined, the connected wires can be identified. As it was noted in Chapter I, each end segment can be considered to have zero current, unless it is physically connected to another wire. The wire end segments can be identified by the use of an array, where a non-connected end is indicated by a 0 and a connected end by a 1. Junctions are identified by assigning the same "junction number" to all of the wire segments that are part of the particular wire junction.

2. Matrix Assembly

Each wire has now been defined, as have the current and charge segments associated with their respective wires. The translation of local to global coordinates now allows (Eq. 2-15), (Eq. 2-16), (Eq. 2-17) and (Eq. 2-18) to be evaluated for each wire segment. These Green's function integrals are then used in the matrices defined in (Eq. 2-36). When evaluating the Green's function integrals, the determinant must be tested and wire ends identified.

Terms can be added to the matrices A and B to account for lumped wire loading. Since the A matrix represents the magnetic potential integral, inductive loading can be added to the A matrix. The inductive lumped element loading is added to the real part of A:

$$Ar = Ar + \frac{1}{30}L \qquad \text{(Eq. 3-1)}$$

where L represents a diagonal matrix the size of A whose diagonal values are the lumped element inductances of each segment.

The capacitive and resistive lumped element loading can be implemented by adding diagonal matrices to the B matrix. The lumped capacitors are added to the real part of the B matrix, while the lumped resistances are added to the imaginary part of the B matrix:

$$Br = Br - \frac{1}{30}\frac{1}{\left(\frac{vo}{\Delta l}\right)}Creciprocal \qquad \text{(Eq. 3-2)}$$

$$Bi = Bi - \frac{1}{30}R. \qquad \text{(Eq. 3-3)}$$

The B_r matrix needs to be further augmented to account for the potential of each wire end. Assigning each wire a start and stop end in reference to the assumed direction along the local axis and creating a matrix of negative and positive 1's to indicate the respective end type, the B_r matrix can be augmented with the newly created end potential matrix. This augmented matrix now accounts for all electric scalar potential effects.

3. KCL and KVL for Wire Ends

Two conditions, KCL and KVL, must be imposed on each wire end. KCL implements the continuity of current at a wire junction, and KVL implements the continuity of potentials. When a wire end is not connected, KVL need not be imposed since a zero end current can be assumed in the MOM model. KCL and KVL can be imposed by augmenting the B_r matrix. Because the number of KCL and KVL equations equals the number of wire ends, the augmented matrix will be square.

4. Super-Matrix Assembly

Now that all of the matrices have been modified to account for lumped loading, wire end potentials and KVL and KCL, the super-matrix can be assembled with respect to (Eq. 2-49). In order to accomplish this matrix assembly, the B_r matrix needs to be inverted, but due to the nature of the rest of the algorithm, only the upper left corner of the inverse is needed. The super-matrix can now be solved for the eigen values, which in turn give the model's resonant frequencies.

5. Presentation of Results

The results are presented for eigen frequencies (numerical values) and their associated eigen currents and far-fields. MATLAB graphics features are used as will be shown in the next section.

The following section verifies the eigen problem formulation, comparing computer solutions to the analytic solutions.

B. VERIFICATION FOR A SINGLE WIRE

The eigen theory and its computer implementation can now be tested. The theory and the eigen code can be verified by solving for the resonance frequencies of an object which has a known analytic eigen solution and comparing these two sets of solutions. For example, a single thin wire is an object of simple geometry with known resonance frequencies, which can be found using:

$$f_n = n\frac{c}{2L}\left[1 - \frac{\int_0^{2\pi n}\frac{\sin(\tau)}{\tau}d\tau}{2\pi(2\ln(\frac{L}{a}))}\right] \qquad \text{(Eq. 3-4)}$$

where L indicates the length of the wire, a denotes the wire radius and n represents the resonance number. [Ref. 3]

For the computer solution the model needs to first be entered and segmented to indicate current and charge pulses. Segmenting a two meter long wire into twelve charge segments, the model appears as in (Fig. A-1). The eigen program is then run, and the resonance frequencies are compared with the known resonance frequencies from (Eq. 3-4).

	Frequency		
Resonance Mode	**Equation (E3-4)**	**Eigen Code**	**Percent Difference**
1	73.98 MHz	76.48 MHz	3.3%
2	147.9 MHz	143.9 MHz	2.8%

The computer solutions for the first two resonance frequencies of the thin wire are very close to the analytic solutions.

As noted in the previous section, the eigen program provides additional results. The eigen vectors represent the current distributions at the resonant frequencies. The magnitudes of the surface currents for the first two resonances are shown in (Fig. A-2) and (Fig. A-3). The red regions indicate strong currents and the blue regions indicate weak current. It is clear that the first resonant frequency has a current peak at the center, akin to the half-wavelength dipole mode. The second resonance frequency has two symmetric peak current regions off center, akin to the full wavelength dipole mode.

Each eigen vector, or eigen current, has an associated electromagnetic field. Of particular interest are the far-field patterns for each eigen frequency. These fields (for the single thin wire) can be displayed as total field magnitude, (Fig. A-4) and (Fig. A-5), or as the field magnitude for specific polarizations such as horizontal, (Fig. A-6) and (Fig. A-7). The plots can have a section cut away to provide a better view of how the object is oriented in relation to its field, as demonstrated for the first eigen frequency in (Fig. A-4) and (Fig. A-6). Each of these field plots can be displayed in either three dimensions or as a polar plot in each of the major planes as in (Fig. A-8), (Fig. A-9), (Fig. A-10), (Fig. A-11), (Fig. A-12) and (Fig. A-13). Additionally, a far-field sphere plot, (Fig. A-14) and (Fig. A-15), can show the far-field magnitude, with the sphere's color indicating the magnitude in that particular direction.

This chapter has provided the basics of implementing eigen theory into a computer code. The eigen formulation and its computer code implementation were then successfully verified for a simple object. The next chapter addresses the task of finding resonant frequencies for complex objects.

IV. EIGEN ANALYSIS FOR COMPLEX OBJECTS

In order to demonstrate the computer eigen analysis for complex metallic objects, two examples are provided. The first example is of a PEC sphere for which the resonant frequencies are known. This allows for a second check of the accuracy of the eigen code. The second example is a Cessna aircraft. It is far more complex and is an example of an object of practical interest.

A. CONDUCTING SPHERE

A sphere is a good example of a complex object for which the resonance frequencies are known. A sphere also has some properties which require it to be handled by the eigen code in a slightly different manner. It is obvious that a perfect sphere is symmetrical with respect to any axis through the sphere's center. A configuration that appears symmetric in that manner has multiple eigen vectors at the same eigen frequency. This is called "mode degeneracy" and causes errors in the eigen solution. In fact, the sphere is the worst case because of its perfect symmetry. To avoid the mode degeneracy problem, the eigen algorithm can be adjusted toward a correct solution by making the wire grid model of the object slightly asymmetric. This will cause "separation" of the degenerate eigen modes and result in a number of modes with very close eigen frequencies. The size of the eigen frequency "clusters" will be proportional to the amount of asymmetry introduced to the wire grid model. The eigen frequencies in a cluster can be averaged to generate the best approximation of the natural resonance frequencies of the object, thus circumventing the mode degeneracy.

The assembly of the wire grid model for a sphere provides insight into the MOM's use of wire and segment spacing. In order to increase the accuracy the segment lengths should be roughly equal; otherwise, the resultant matrix may be ill-conditioned. The sphere's wire grid model used for this simulation is shown in (Fig. A-16).

A final consideration for running the eigen analysis for a sphere is the concept of DC blocking. For any eigen problem where "loops" exist, there is a trivial solution for the eigen values of zero. The trivial solution exists when the wire grid structure forms a complete path, connecting all ends into a circle. This configuration allows for a DC current to become an eigen vector at the zero eigen frequency. The existence of the zero eigen value results in a very large conditioning number indicating an ill-conditioned matrix. Capacitors can be added to block the DC current. These capacitors are included in the model per (Eq. 3-2), and if their reciprocals are kept to a minimum in value, they will have little effect on the results other than the removal of the zero eigen value.

The eigen frequencies of the sphere can be derived from the equation:

$$\nu = \frac{\rho}{2\pi a}\sqrt{\varepsilon\mu} \qquad \text{(Eq. 4-1)}$$

where ρ represents the characteristic values of a sphere, a is the sphere's radius and the medium surrounding the sphere is described by ε and μ. [Ref. 4]

The radar cross section (RCS) of a sphere in the Mie region, also provides an estimation of its resonance frequencies. [Ref. 5]

After entering the perturbed sphere into the eigen program and running the simulation, the eigen frequencies produced by the simulation for a radius of .5 m can be compared to those from (Eq. 4-1) and from [Ref. 5] (Sphere RCS vs. Frequency).

Resonance Mode	Frequency Equation (E4-1)	Eigen Code	Percent Difference
1	82.12 MHz	91.7 MHz	11.7%
2	154.7 MHz	189.9 MHz	22.8%

Resonance Mode	Frequency RCS from [Ref. 5]	Eigen Code	Percent Difference
1	95.4 MHz	91.7 MHz	4.2%
2	217.4 MHz	189.9 MHz	12.6%

The computer eigen solution provides the current density and the total electric field pattern for each eigen frequency. These plots are provided for the first eigen frequency as (Fig. A-17) and (Fig. A-18). The total radiated field with a cutout can be seen in (Fig. A-19). The plots show the dipole-like far-field pattern for the sphere's first mode. It should be kept in mind that more than one eigen current exists for this mode due to the sphere's symmetry. However, all eigen currents for the same eigen frequency can be obtained through rotation from each other by an "orthogonal" angle. The accuracy of the eigen solution can be improved by increasing the number of wires in the sphere's wire grid model at the expense of increasing computer time and required memory. The next section will show that the eigen code can handle objects of even greater complexity.

B. ELECTROMAGNETIC RESONANCE OF AN AIRCRAFT

In a more practical sense, the objects for which resonance frequencies are needed are more complex than a thin wire or a sphere. The eigen code is capable of solving for the eigen frequencies and eigen currents of complex objects. As an example, the eigen code has been used to determine the resonance frequencies for the wire grid model of a Cessna aircraft for which there is no analytic solution.

The eigen code is applied to the wire grid model of the Cessna aircraft, (Fig. A-20), to determine the resonance frequencies, the first four of which are shown in the table below:

Resonance Number	Resonance Frequencies
1	8.282 MHz
2	8.333 MHz
3	12.51 MHz
4	18.35 MHz

These frequencies are of interest in detecting the aircraft using HF radar, for example. Looking solely at the first eigen frequency, the current density on the aircraft, (Fig. A-21), produces the total field pattern displayed in (Fig. A-22). From these graphs, it is clear that the aircraft wings cause the first resonance, and the corresponding field is similar to that of a dipole in the plane of the front edge of the aircraft wings.

The eigen algorithm has proved its ability to find eigen frequencies and eigen currents for complex objects. In the following chapter, the eigen process will be summed up, and recommendations will be made as to further research in this area.

V. CONCLUSIONS AND RECOMMENDATIONS

Computational electromagnetics provides solutions to radiation and scattering problems for bodies which are too complex in shape to solve for using analytic techniques. The MOM technique allows one to form a matrix description of radiation or scattering by a conducting object. The resulting matrices, which represent the electromagnetic model of the object, can then be manipulated into a standard algebraic eigen value problem whose solutions are the resonance frequencies of the model.

Testing of the computer eigen code for both simple and complex objects indicates that the computer results are good approximations of the resonance frequencies. The eigen currents associated with each eigen frequency show different regions of the object which contribute to that particular eigen frequency.

The eigen code can be used for a number of applications such as determining an object's usefulness as an antenna or finding the frequencies of maximum scattering for a metallic object. In its current stage of development, the code is capable of finding resonance frequencies for complex objects, but the complexity of an object is directly proportional to the amount of difficulty in running the simulation with respect to memory requirements and speed. A more detailed electromagnetic model produces a closer approximation of an object's resonances, but at the expense of increasing required memory and computation time.

Additional work can be done in determining faster and more efficient methods for matrix manipulation, such as eliminating the inversion of the full augmented matrix B_r and implementing iterative eigen solvers to find only a limited number of eigen frequencies.

These goals are feasible and their completion will contribute to increasing the scope of eigen analysis applicability.

APPENDIX. EIGEN ANALYSIS FIGURES

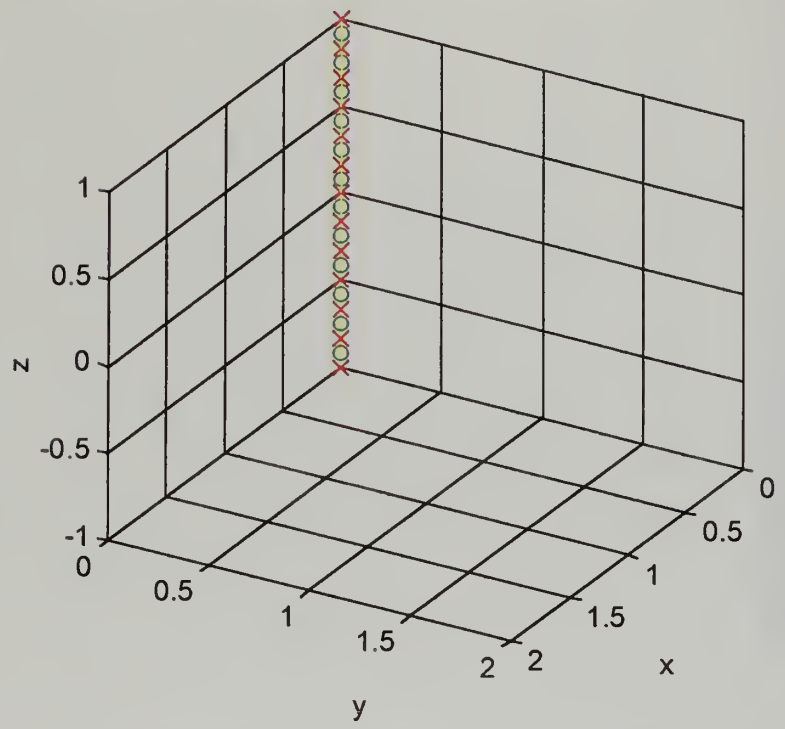

Figure (Fig. A-1), Segmented thin wire model

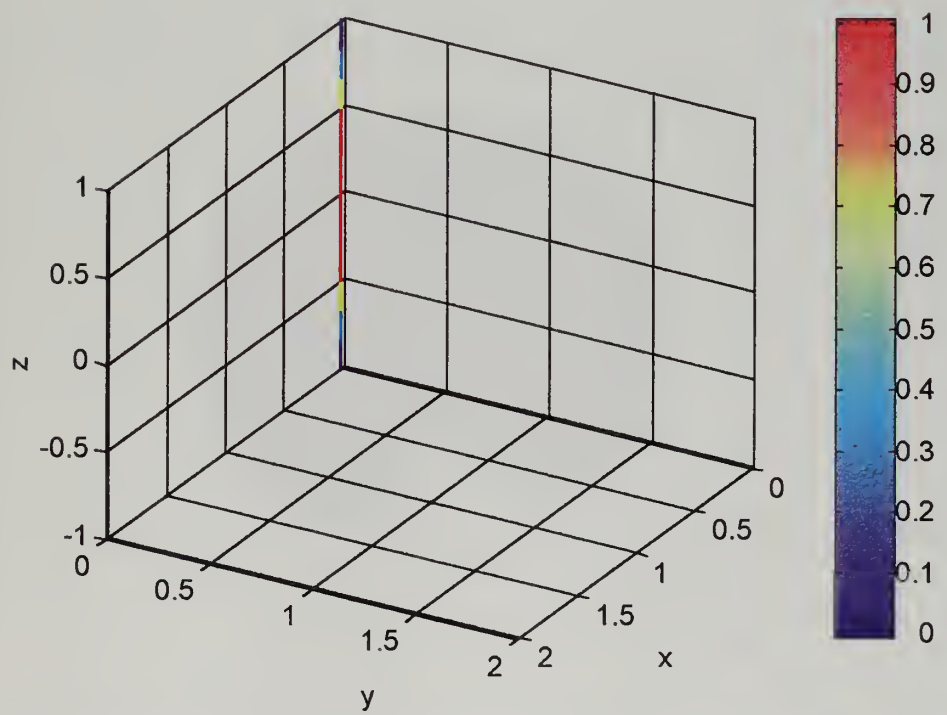

Figure (Fig. A-2), Current magnitude for the thin wire model at 76.48 MHz

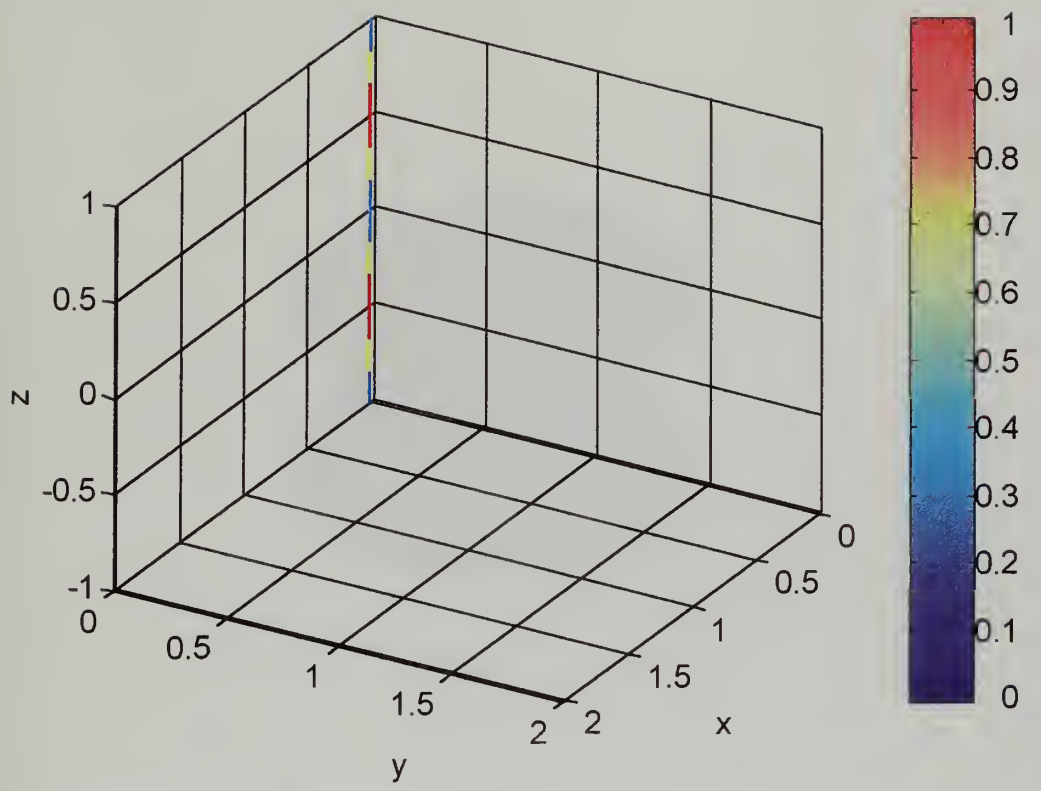

Figure (Fig. A-3), Current magnitude for the thin wire model at 143.9 MHz

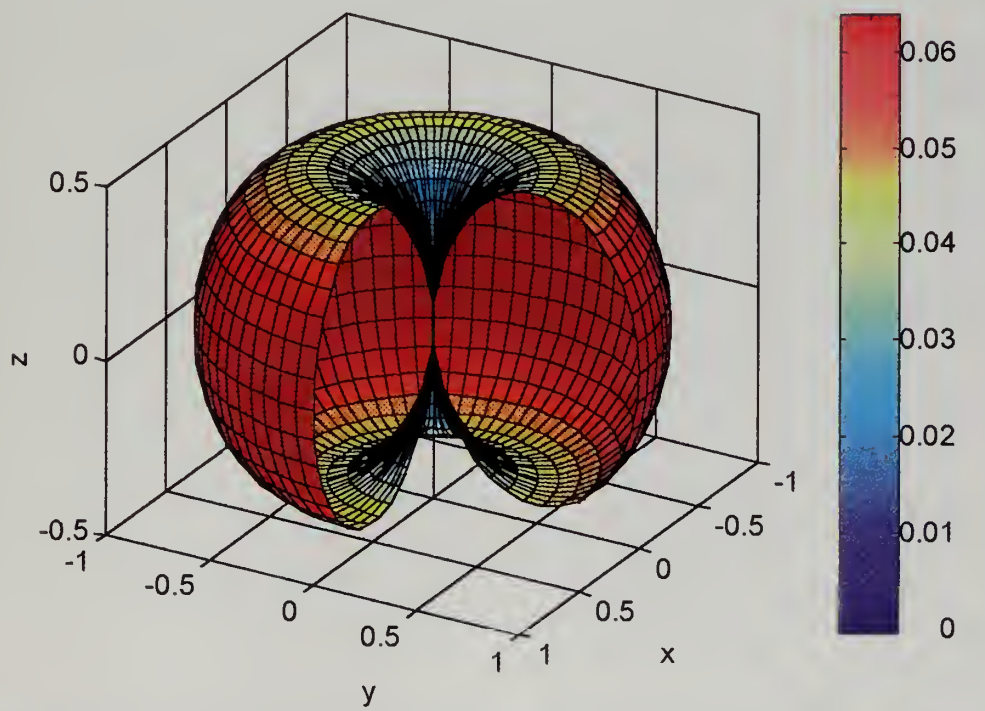

Figure (Fig. A-4), Total field magnitude for the thin wire model at 76.48 MHz

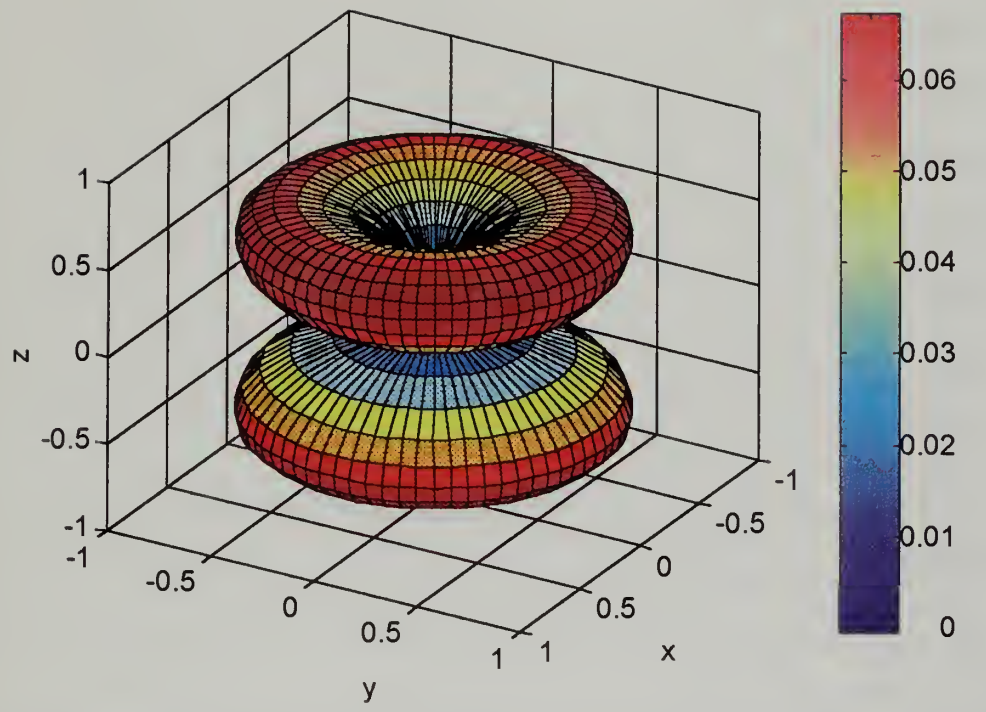

Figure (Fig. A-5), Total field magnitude for the thin wire model at 143.9 MHz

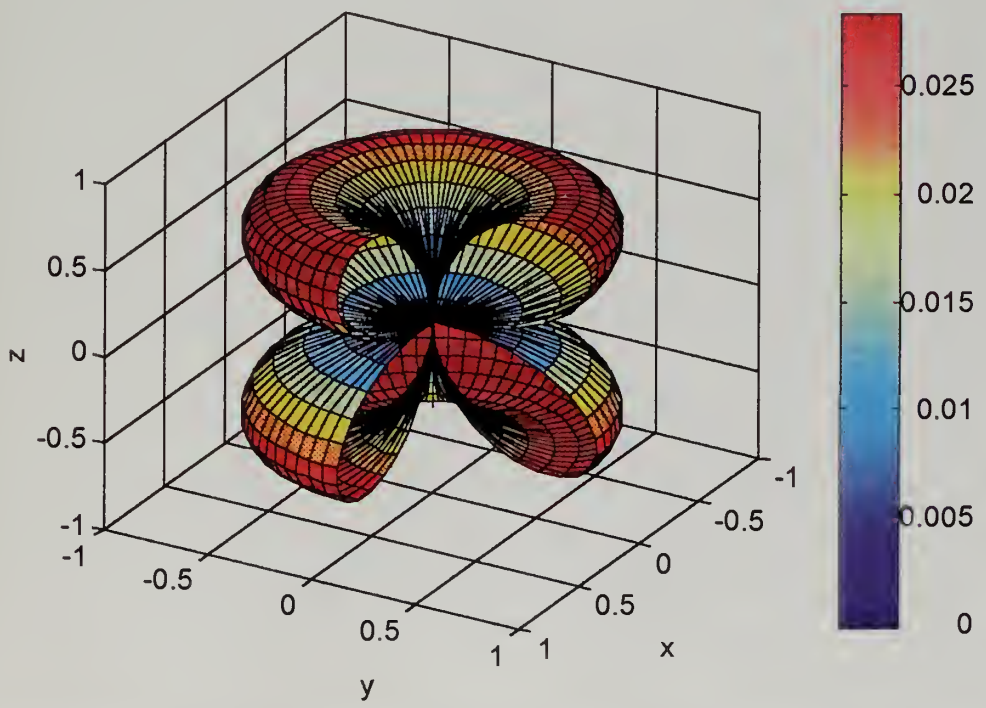

Figure (Fig. A-6), Horozontal field magnitude for the thin wire model at 76.48 MHz

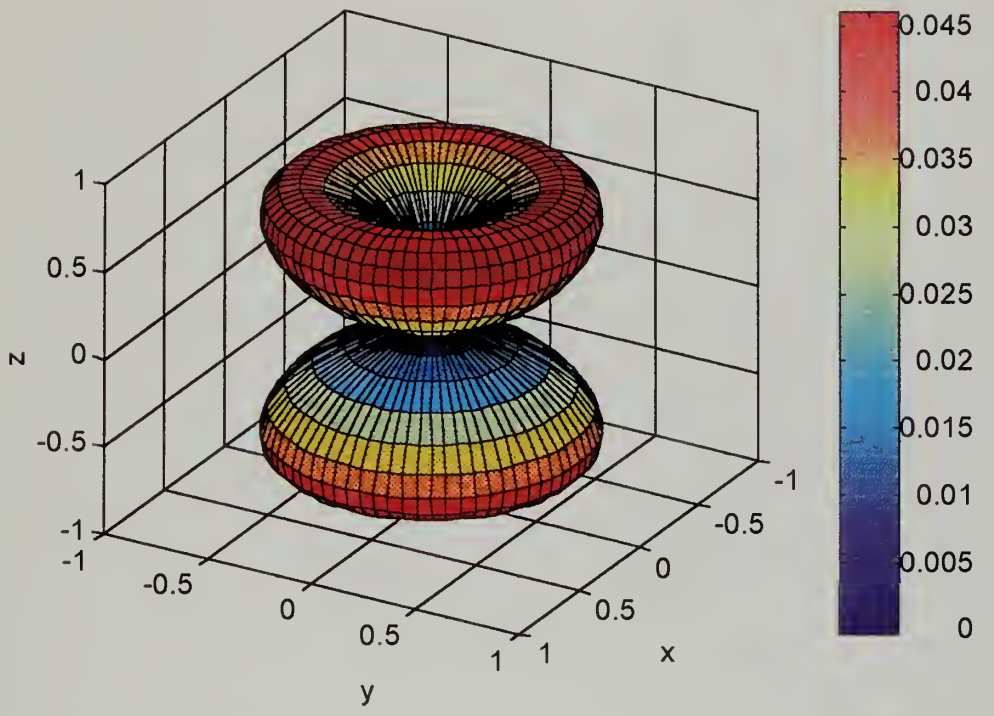

Figure (Fig. A-7), Horozontal field magnitude for the thin wire model at 143.9 MHz

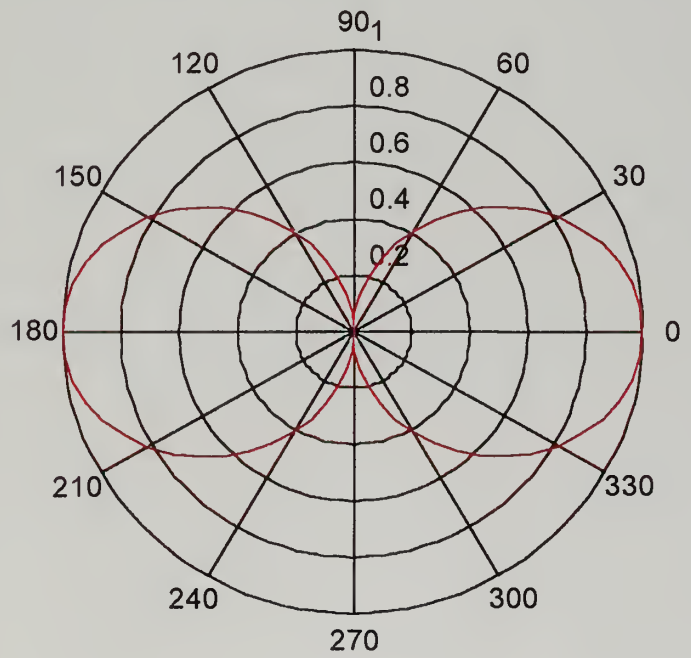

Figure (Fig. A-8), XZ plane polar plot for the thin wire model at 76.48 MHz

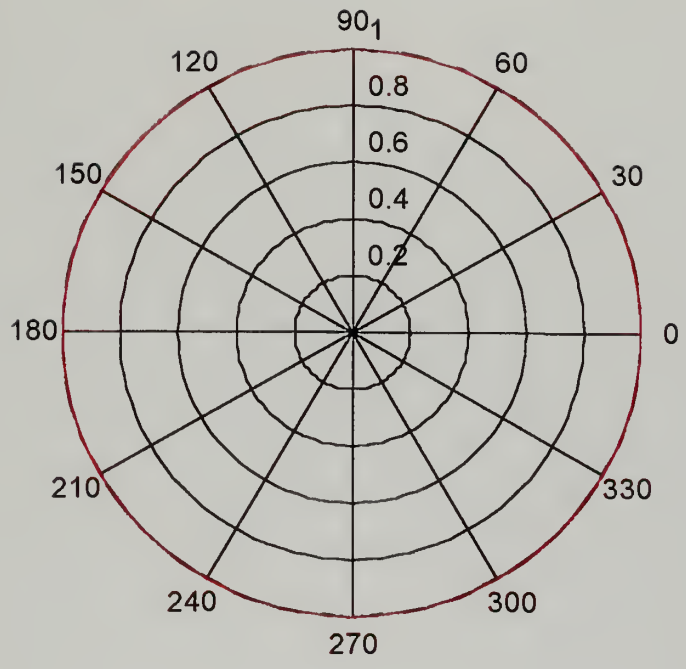

Figure (Fig. A-9), XY plane polar plot for the thin wire model at 76.48 MHz

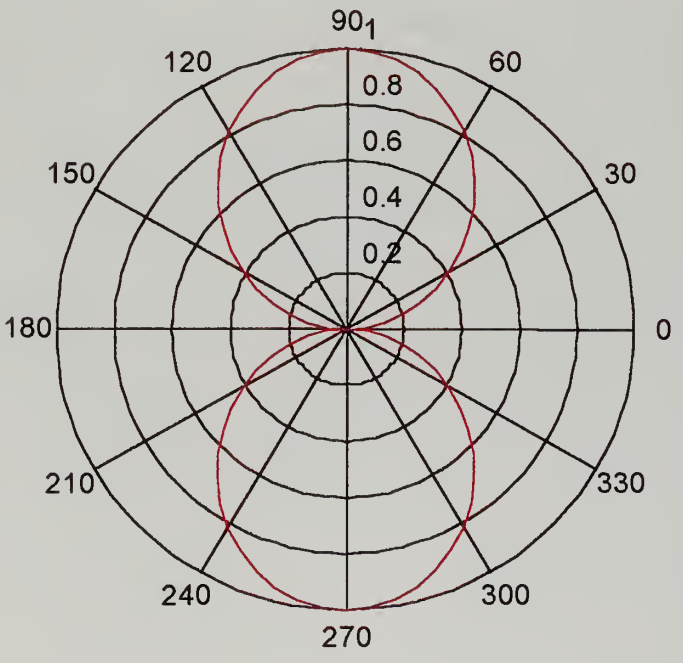

Figure (Fig. A-10), YZ plane polar plot for the thin wire model at 76.48 MHz

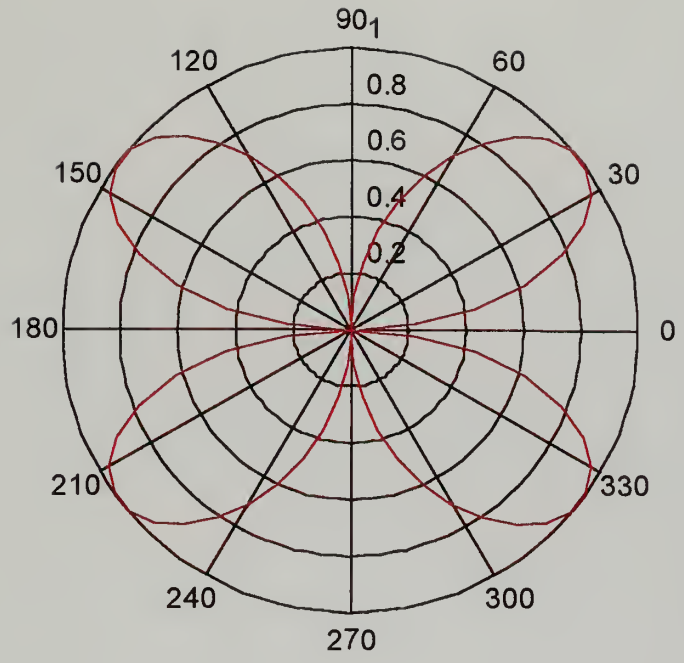

Figure (Fig. A-11), XZ plane polar plot for the thin wire model at 143.9 MHz

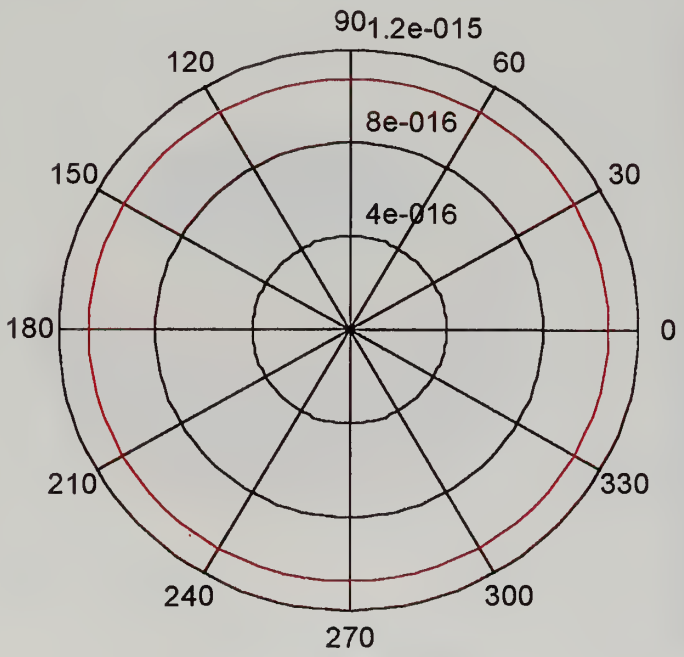

Figure (Fig. A-12), XY plane polar plot for the thin wire model at 143.9 MHz

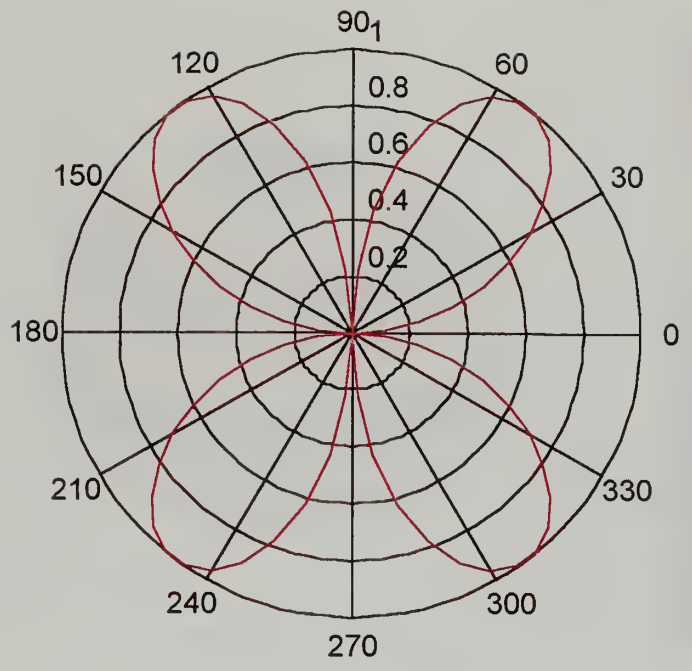

Figure (Fig. A-13), YZ plane polar plot for the thin wire model at 143.9 MHz

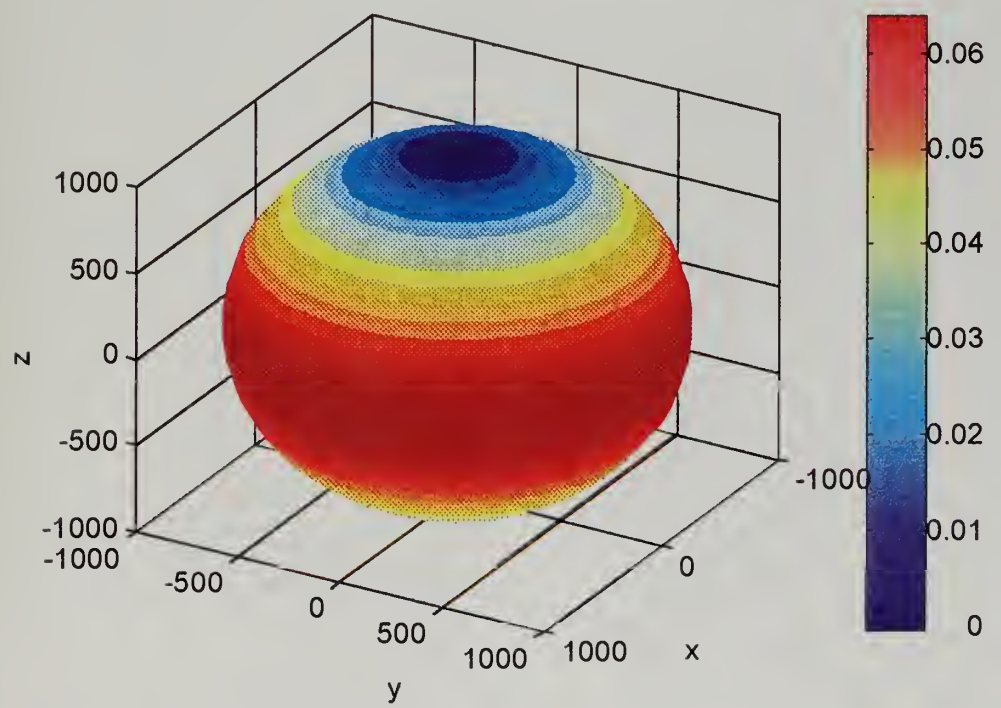

Figure (Fig. A-14), Field magnitude of thin wire model at 76.48 MHz and at a distance of 1000 m

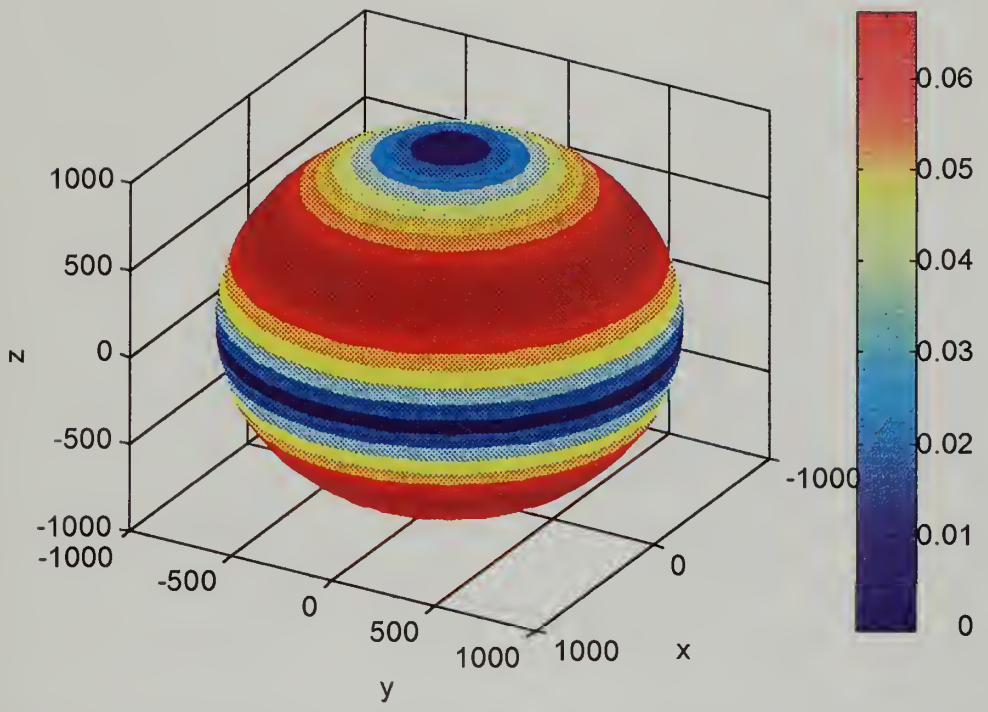

Figure (Fig. A-15), Field magnitude of thin wire model at 143.9 MHz and at a distance of 1000 m

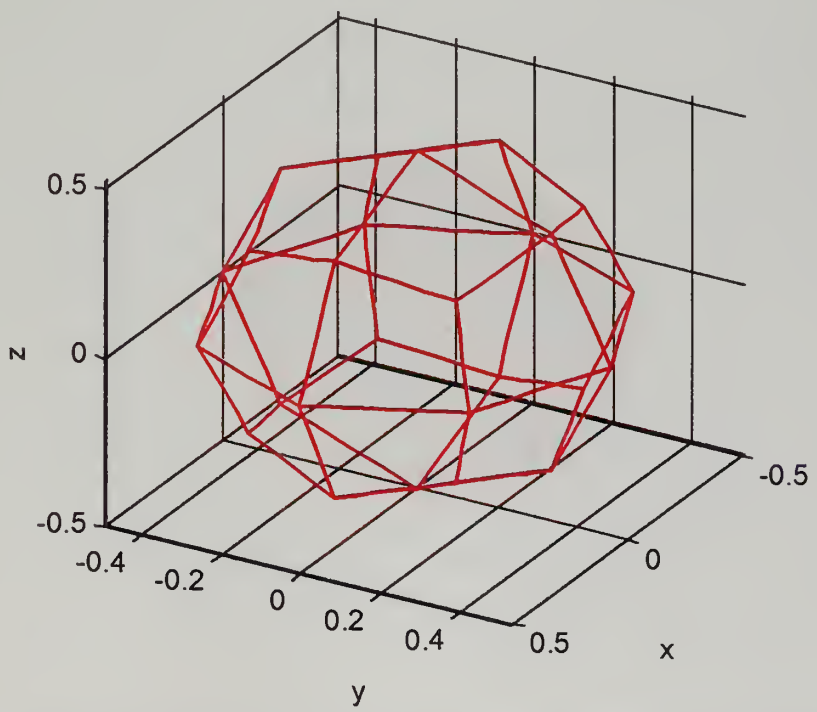

Figure (Fig. A-16), Wire grid segmented sphere model for eigen simulation

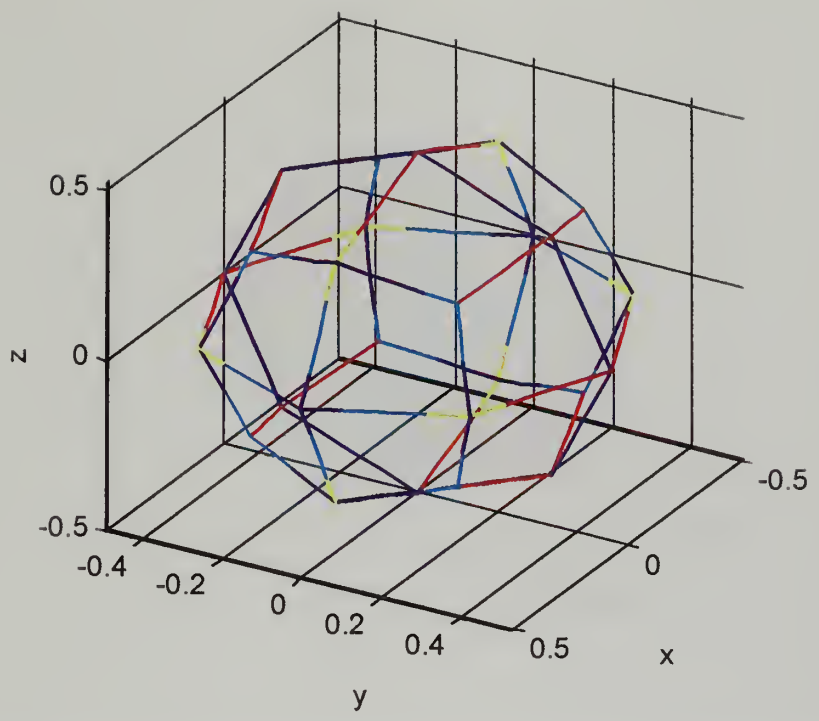

Figure (Fig. A-17), Current density for the first eigen frequency for the sphere

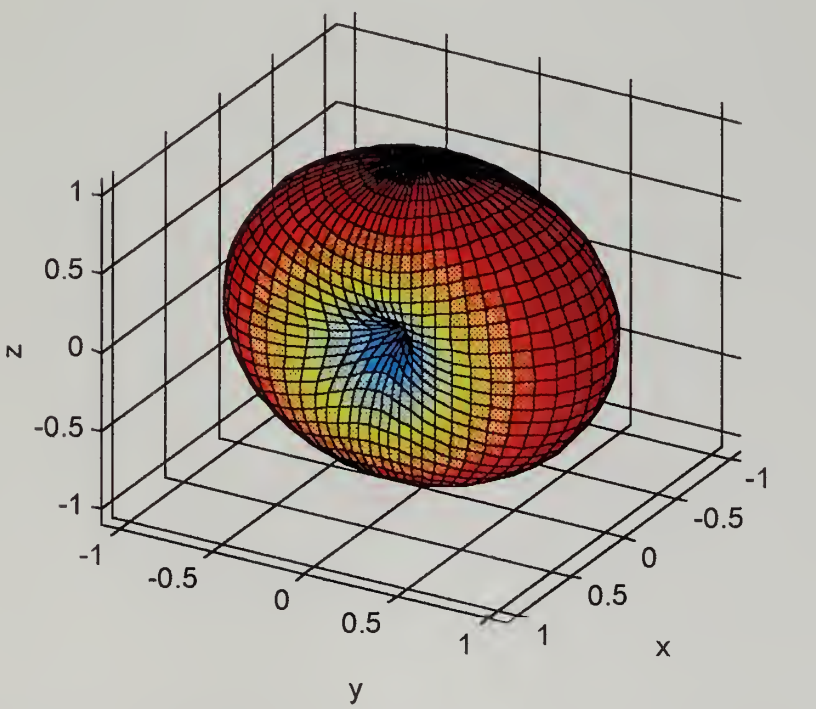

Figure (Fig. A-18), Total electric field pattern for the sphere's first eigen frequency

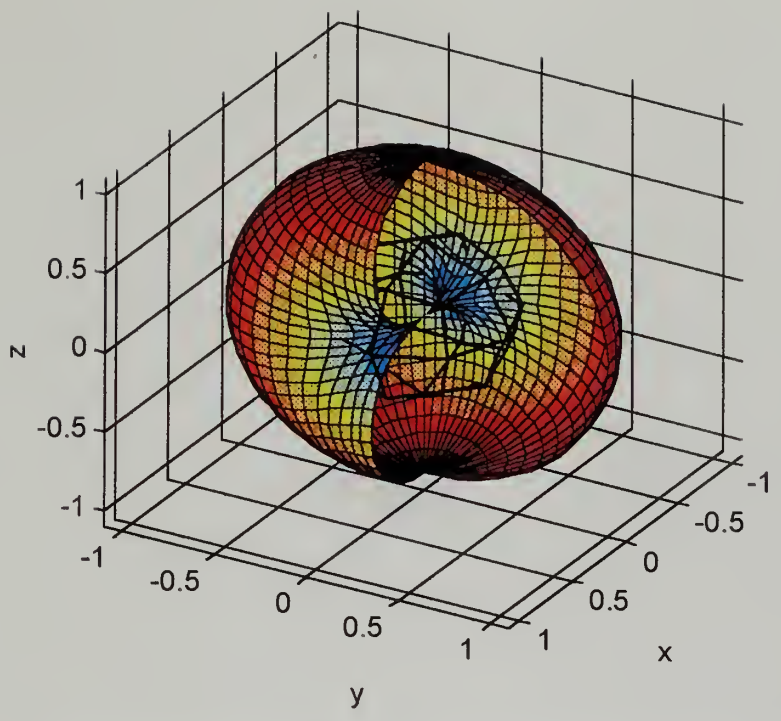

Figure (Fig. A-19), Total electric field pattern for the sphere's first eigen frequency with cut out

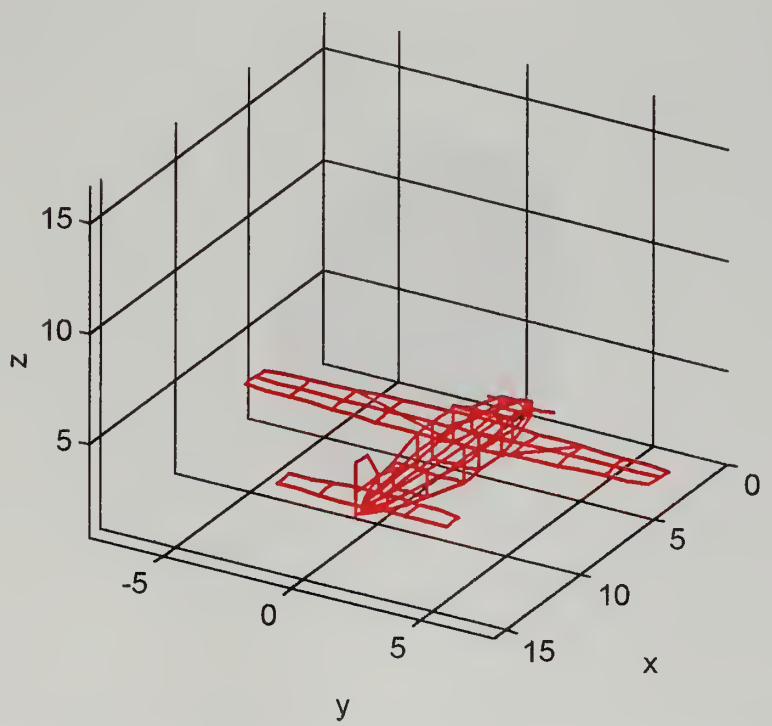

Figure (Fig. A-20), Wire grid Cessna model for eigen simulation

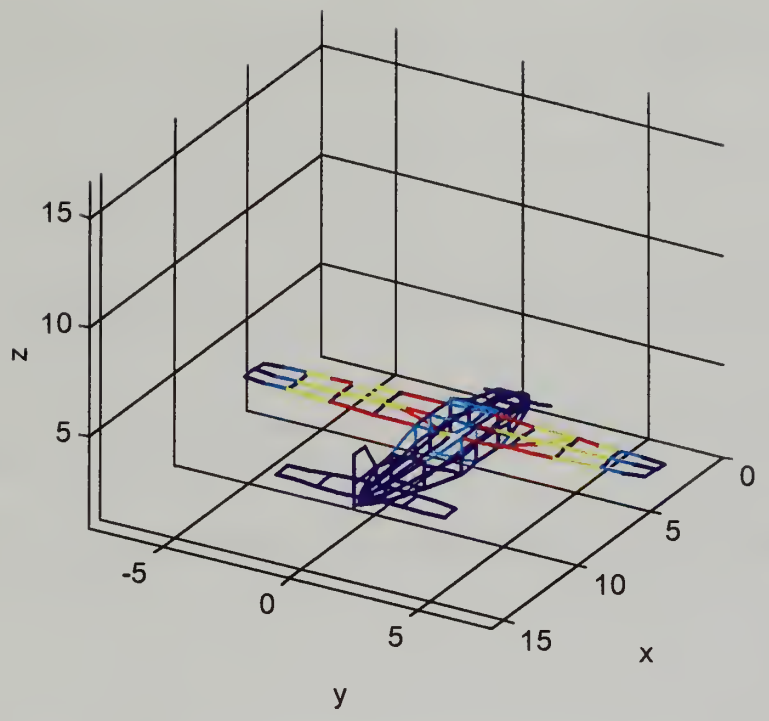

Figure (Fig. A-21), Current density for the first eigen frequency on the Cessna

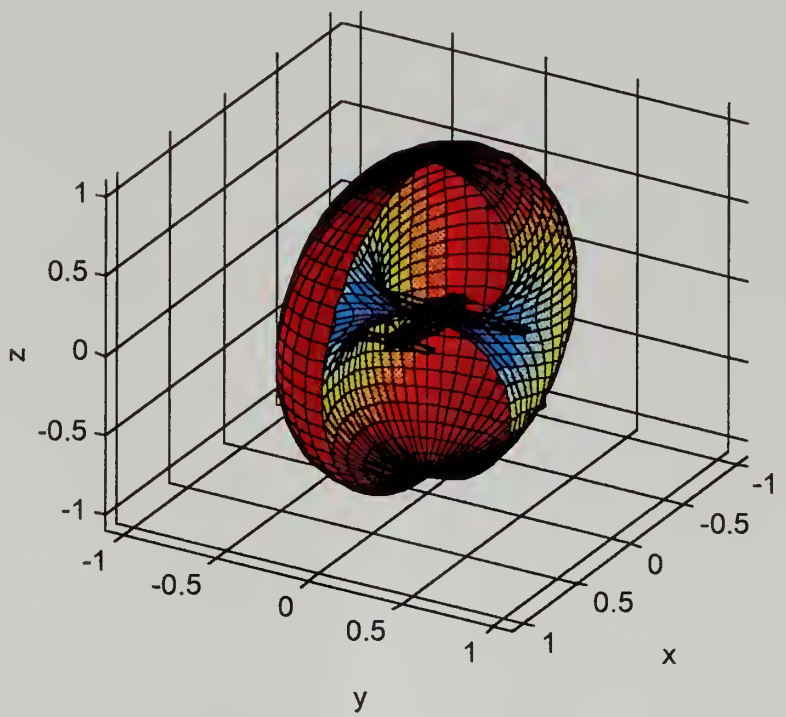

Figure (Fig. A-22), Total electric field pattern for Cessna's first eigen frequency with cut out

LIST OF REFERENCES

1. Tesche, Fredrick M., "On the Analysis of Scattering and Antenna Problems Using the Singularity Expansion Technique," pp.53-55, *IEEE Transactions on Antennas and Propagation*, Vol. AP-21, No. 1, January 1973.

2. Balanis, Constantine A., *Advanced Engineering Electromagnetics*, pp. 670-731, John Wiley & Sons, New York, 1989

3. Van Blaricum, Michael L., "The Natural Resonances of Thin-Wire Structures in Various Configurations," pp. 12-21, Mission Research Corporation, Monterey, CA, June 1977.

4. Stratton, Julius A., *Electromagnetic Theory*, pp.554-563, McGraw-Hill Book Company, Inc., New York, 1941.

5. Skolnik, Merrill I., *Introduction to Radar Systems*, pp.33-34, McGraw-Hill, Inc., New York, 1980.

INITIAL DISTRIBUTION LIST

1. Defense Technical Information Center 2
   8725 John J. Kingman Rd., Ste 0944
   Ft. Belvoir, VA 22060-6218

2. Dudley Knox Library 2
   Naval Postgraduate School
   411 Dyer Rd.
   Monterey, CA 93943-5101

3. Chairman, Code EC 1
   Department of Electrical and Computer Engineering
   Naval Postgraduate School
   Monterey, CA 93943-5121

4. Professor Richard W. Adler, Code EC/Ab 5
   Department of Electrical and Computer Engineering
   Naval Postgraduate School
   Monterey, CA 93943-5121

5. Professor Jovan E. Lebaric, Code EC/Lb 2
   Department of Electrical and Computer Engineering
   Naval Postgraduate School
   Monterey, CA 93943-5121

6. Commander Gus Lott, Code EC/Lt 1
   Department of Electrical and Computer Engineering
   Naval Postgraduate School
   Monterey, CA 93943-5121

7. Commanding Officer 1
   (ATTN: Code 30, CDR Zellmann)
   Naval Information Warfare Agency
   9800 Savage Rd.
   Ft. Meade, MD 20755-6000

8. LeeAnn Enriquez 1
   5709 Evergreen Knoll CT
   Alexandria, VA 22393